Numerical Simulation and Verification of Mechanical Noise Generation in Combustion Engines

H.H. Priebsch, H. Herbst, G. Offner, M. Sopouch
Christian Doppler Lab of Engine and Vehicle Acoustics,
Inst. for Combustion Engines, TU Graz, Austria and
AVL List GmbH, Graz, Austria
e-mail: hans-herwig.priebsch@accgraz.com

Abstract

In several speed and load ranges of car engines the generation of mechanical noise contributes significantly to the overall engine noise. The numerical simulation of mechanical noise requires precise models for both the noise source and for the transfer path to the radiating surface.

The paper describes two typical examples of simulation models for the generation mechanisms of mechanical noise: The noise generated by the timing drive (chain drive) and the piston slap induced noise. After describing the theoretical background for relevant mathematical models, examples of characteristic results are given. The contributions to overall engine structure borne noise are discussed.

Finally, simulation results are compared to experimental data. The problem of measuring significant dynamic components in the noise generation areas is discussed and possibilities for validating simulation results by comparing them with measured ones are shown.

1 Introduction

The efficiency in developing new engines and power trains for modern vehicles can be significantly improved by capable prediction methods. There are various prediction requirements in the development process of an engine. Among these, the prediction of engine noise is still one of the most challenging due to the specific and complex simulation models required for precise results.

Engines and power units are still a significant source for noise pollution in the urban environment. Besides combustion noise, the noise generated by mechanical contacts of the moving and vibrating parts in engine contributes to the overall engine noise. Depending on the engine operating condition, this mechanical noise may become the dominating part even in the high speed range of engines.

Since over 20 years, the Finite Element Method (FEM) has been used for vibro-acoustic analyses of engines. Although FEM is of high value for linear structure vibro-acoustic models, the method is not sufficient to model the rotating and oscillating parts and their highly non-linear contact events in an engine.

Thus, hybrid calculation procedures are often required, combining very large FEM models, multi-body properties and specific equations for local contact events. There are two specific challenges of such simulation tasks. On one hand, the stiff system of equations generated due to different contact characteristics require different solvers for optimum solution time and high quality results. Despite of a number of international efforts to develop a common simulation methodology, e.g. [2], there is still no sufficient solution existing. On the other hand, the validation of the calculated results by means of experimental ones is of high complexity. Often, primary components e.g. contact forces in moving systems can not be measured from tests. Secondary components e.g. surface velocities, etc. have to be selected carefully to enable for tuning system parameters of the original simulation model.

This paper shows two typical applications in this research topic and the quality of achievable results. The first application example deals with the timing drive, the second with the piston to liner contact. Due to the different contact characteristics, two

different solutions are shown. After the description of methods and models the calculated results and efforts for validation are described. Ways of further improvements are discussed, also.

2 Basic equations

Two modelling methodologies are described: One for the simulation of a chain driven timing drive and a second for the piston secondary motion.

2.1 Rigid bodies and elastic contacts

For specific applications e. g. timing drives of engines the assumption of relative rigidity of the moving parts compared to the elasticity of the can be made. The simulation of body motion and contacts between chain, sprockets and guides is based on the following equations:

2.1.1 Rigid body equation

In this case equation (1) may be used

$$\boldsymbol{M}_{comp} \cdot \ddot{\boldsymbol{q}}_{comp} = \boldsymbol{f}^{(a)}_{comp} + \boldsymbol{f}^{*}_{comp} \tag{1}$$

where $\boldsymbol{M}_{comp}$ is the matrix of masses and moments of inertia for a specific engine component, $\ddot{\boldsymbol{q}}_{comp}$ denotes the six degrees of freedom of the rigid body accelerations with reference to the engine components centre of gravity. The right hand side of the equation contains external loads $\boldsymbol{f}^{(a)}_{comp}$ and joint forces and moments $\boldsymbol{f}^{*}_{comp}$. External loads (e.g. gas force) and moments are functions given in time, that are determined from given measurement data. The non-linear terms of excitation loads in contacts are given by joints equations, connecting one body to another (e.g. chain`s bush to sprocket).

Applying the simplifications:

- Principle axis of inertia agree with the axis of the local (body fixed) co-ordinate system: the matrix of masses and moments of inertia become a diagonal matrix ($\boldsymbol{M}_{comp} = diag(\boldsymbol{M}_{comp})$).

- Rotational motion components related to local co-ordinate system (Eulerian approach): time invariance of inertia tensor ($\boldsymbol{M}_{comp} = const.$)

as well as the extension to a system of rigid engine components (The number of components is n_{comp}.)

$$\boldsymbol{M}_{system} \cdot \ddot{\boldsymbol{q}}_{system} = \boldsymbol{f}^{(a)}_{system} + \boldsymbol{f}^{*}_{system} \tag{2}$$

leads to a fully de-coupled ODE-system. Hence, accelerations $\ddot{q}_{system,i}$ of each generalised co-ordinate can be expressed by a simple scalar equation:

$$\ddot{q}_{system,i} = \frac{f^{(a)}_{system,i} + f^{*}_{system,i}}{M_{system,i}} \tag{3}$$

where $M_{system,i}$ denotes engine components masses or moments of inertia respectively. i ($1 \le i \le 6 \cdot n_{comp}$) is the index of the main diagonal element of $\boldsymbol{M}_{system}$ as well as of the corresonding force-vector-component.

The integration of (3) is performed in time domain using e.g. a predictor/corrector method where the deviation between predictor (explicit) and corrector (implicit) is utilised for an automatic step size control. Due to the high non-linearity of the investigated systems, a root finder algorithm to detect state events (e.g. impacts and separations in contacts) is applied. Typical applications with frequent state events require a comparatively small time step size (typically 10^{-8} s) in order to achieve sufficient convergency.

2.1.2 Contact of solids equation (elastic foundation model)

The determination of contact forces $\boldsymbol{f}^{*}_{comp}$ based on the knowledge of profile's interference of two solids (rigid bodies) usually requires the solution of an integral equation for the pressure. Taking into account the huge amount of contact pairs which arise in the timing drive domain (e.g. contact of chain to sprockets and guides) there is a strong request for a simplified contact approach. Thus, a simple Winkler elastic foundation ("mattress") is used (Fig.1). Since the magnitudes of the single contact forces are moderate at chain drives and the influence of a particular contact on the entire system's behaviour is minor, a simplified contact approach leads to a reasonable approximation.

The representation of the profile's shape is done by means of bezier-splines (restricted to plane

contours). Taking into account the contact profile as a sum of the two body profiles $z_i(x)$ and $z_{i+1}(x)$

$$\tilde{z}_{i,i+1}(x) = z_i(x) + z_{i+1}(x), \quad (4)$$

the normal elastic displacements $u_{\tilde{z},j}$ of a discrete section j within the contact area is given by

$$u_{\tilde{z},j}(x) = \begin{cases} \delta - \tilde{z}_{i,i+1}(x), & \delta > \tilde{z} \\ 0, & \delta \le \tilde{z} \end{cases} \quad (5)$$

$\delta = \mathbf{z} \circ (\mathbf{q}_i - \mathbf{q}_{i+1})$ ..... penetration at origin

$\mathbf{z}$ ..... contact direction

The contact pressure p_j in any section depends on the deformation of that section only, and can be expressed by

$$p_j(x) = (K_E / h) \cdot u_{\tilde{z},j}(x) \quad (6)$$

where K_E denotes the elastic modulus of the foundation and h its depth. The required contact force $F_{\text{contact i,i+1}}$ is finally obtained by integrating the pressure distribution. Accumulation of all contact forces acting on a specific engine component leads to the force component $\boldsymbol{f}^*_{comp}$, as indicated in equation (1).

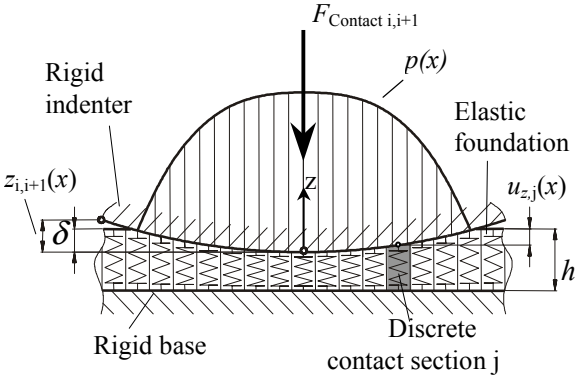

Figure 1: Elastic foundation model (Winkler mattress).

2.2 Vibration equation and lubricated contacts

The second set of equation is used in case the elastic vibrations of the contacting parts effect the contact event itself considerably. The basic ideas of this method were published in [1]. The relevant formulas and models have been refined and extended continuously and several specific applications for hydro-dynamic contacts in the engine bearings and between piston and liner have been described [3, 4].

Because of the complex structure of a multi-body-system, the total system has to be broken down into coupled systems, consisting of bodies, e.g. piston and liner, with linear elastic behaviour and connections, e.g. lubricated regions, considering the non-linear forces, acting between the connected bodies. The mathematical modelling of these sub-systems is done via the corresponding equations:

- Vibration equation for small motions (vibrations) of bodies
- Equations of big (global) motions of each body
- Non-linear contact equations to compute forces and moments, acting between connected bodies

The formulation of the particular equations as well as the introduction of ingenious simplifications will be resumed in the following section.

2.2.1 Vibration equation

For the calculation of motions each body is represented by a sufficiently high number of sub-bodies (partial masses). The dynamic behaviour of each of these rigid partial masses is given by the classical equation of motion for linear systems derived from the equations of momentum and angular momentum:

$$\boldsymbol{M} \cdot \ddot{\boldsymbol{q}} + \boldsymbol{D} \cdot \dot{\boldsymbol{q}} + \boldsymbol{K} \cdot \boldsymbol{q} = \boldsymbol{f} \quad (7)$$

$\boldsymbol{q} = [\boldsymbol{q_1}, \boldsymbol{q_2}, ..., \boldsymbol{q_n}]^t$ is the generalised displacement vector for n partial masses. Each vector element is a vector itself with three translatorial and three rotational components of motion ($\boldsymbol{q_i} = [u_1, u_2, u_3, \gamma_1, \gamma_2, \gamma_3]^t_i$). Damping matrices ($\boldsymbol{D}$) are calculated from given mass matrices ($\boldsymbol{M}$) and stiffness matrices ($\boldsymbol{K}$) according to the linear combination $\boldsymbol{D} = \alpha \cdot \boldsymbol{K} + \beta \cdot \boldsymbol{M}$. Here, α and β are constants, derived from structural damping and modal frequencies. The right hand side of (7) contains external loads ($\boldsymbol{f}^{(a)}$) and joint forces and moments ($\boldsymbol{f}^*$) as in (1) and inertia terms ($\boldsymbol{p}^*$):

$$\boldsymbol{f} = \boldsymbol{f}^{(a)} + \boldsymbol{f}^* + \boldsymbol{p}^* \quad (8)$$

The non-linear inertia terms $\boldsymbol{p}^*$ result from the co-ordinate transformation of the equations of momentum and angular momentum from the global co-ordinate system to the body related reference co-ordinate system. They consider the inertia components resulting from global motions of the body. Vector $\boldsymbol{p}^* = \left[\boldsymbol{p}_1^*, \boldsymbol{p}_2^*, ..., \boldsymbol{p}_n^*\right]^t$ consists of n mass related components, where each $\boldsymbol{p}_i^*$ contains a force related sub-vector $\boldsymbol{p}_{F,i}^*$ and a moment related sub-vector $\boldsymbol{p}_{M,i}^*$:

$$\begin{aligned} \boldsymbol{p}_i^* &= \begin{bmatrix} \boldsymbol{p}_{F,i}^* \\ \boldsymbol{p}_{M,i}^* \end{bmatrix} = \\ &= \begin{bmatrix} -m_i \cdot \left[\ddot{\boldsymbol{x}}_B + 2 \cdot \boldsymbol{A}_\Omega \cdot \left(\dot{\boldsymbol{x}}_B + \dot{\boldsymbol{u}}_i\right) + \right. \\ \qquad \left. + \left(\boldsymbol{A}_{\dot{\Omega}} + \boldsymbol{A}_\Omega^2\right) \cdot \left(\boldsymbol{x}_B + \boldsymbol{c}_i + \boldsymbol{u}_i\right)\right] \\ -\Delta \boldsymbol{I}_{C_i} \cdot \ddot{\varphi}_i + \left(\boldsymbol{I}_{C_i} + \Delta \boldsymbol{I}_{C_i}\right) \cdot \left(\dot{\boldsymbol{\Omega}} - \boldsymbol{A}_{\dot{\Omega}} \cdot \boldsymbol{\Omega}\right) + \\ + \left(\boldsymbol{A}_\Omega + \boldsymbol{A}_{\varphi_i}\right) \cdot \left(\boldsymbol{I}_{C_i} + \Delta \boldsymbol{I}_{C_i}\right) \cdot \left(\boldsymbol{\Omega} + \varphi_i\right) \end{bmatrix} \end{aligned} \tag{9}$$

The terms (9) are discussed in [1, 3] in more detail. Due to the high non-linearity of $\boldsymbol{p}^*$ the solution becomes CPU-intensive.

Different considerations of $\boldsymbol{p}^*$, depending on global motion properties of the structural components, are necessary. In case of the elastic piston-to-liner contact simulation, special properties can be considered for both the piston and the cylinder liner. Due to the global motion in stroke direction of the piston, the angular components $\boldsymbol{A}_\Omega$, $\boldsymbol{A}_{\varphi_i}$, $\boldsymbol{\Omega}$, φ_i and the corresponding derivatives in time can be neglected and equation (9) reduces to

$$\boldsymbol{p}_i^* = \begin{bmatrix} -m_i \cdot \ddot{\boldsymbol{x}}_B \\ \boldsymbol{0} \end{bmatrix} \tag{10}$$

Here, m_i is the mass of the i-th partial mass of the piston and $\ddot{\boldsymbol{x}}_B$ is the acceleration of the origin of the piston fixed co-ordinate system. The origin of the liner fixed co-ordinate system is time invariant in the global (engine fixed) co-ordinate system. Thus, for all parts having vibrations only, e.g.: the cylinder liner, $\ddot{\boldsymbol{x}}_B = \boldsymbol{0}$ and the inertia terms can be neglected and become $\boldsymbol{p}^* = \boldsymbol{0}$.

2.2.2 Equations of global motions

The linear elastical engine component is represented via a sufficiently high number of partial masses. The generalised displacements $\boldsymbol{q}$ (chapter 2.2.1) of all partial masses affect the motions of the total body also. These global motions are represented with the vector $\left(x_{B,1}, x_{B,2}, x_{B,3}, \alpha, \beta, \chi\right)^t$, that holds the three translatorial and the three rotational motion components of the reference co-ordinate system of the body. The mass properties of the partial masses with reference to the geometry as well as external loads and joint forces and moments affect the global motion of the component also. Therefore, vector $\left(x_{B,1}, x_{B,2}, x_{B,3}, \alpha, \beta, \chi\right)^t$ is computed from the equations for momentum and angular momentum for the total body as described in [1,3,10].

2.2.3 Mixed lubricated contact equation

Combustion engines have several oil-lubricated contacts e.g. slider bearings, piston to liner contact. In these contacts oil separates the two contacting components. Under conditions of fairly low relative motion of contacting parts and heavy loads mixed lubrication may occur. The local oil film thickness between the surfaces decreases to the value of the mean average roughness. The asperity summits rasp against one another and cause local high pressure loads.

To describe such local effects in terms of hydro-dynamic calculation methodology, [5], would require a sufficient local resolution for the discretisation. To provide such high resolution would cause inefficient CPU times. Therefore, the contribution of asperity contact load to local deformations is separated into two parts: The local asperity deformation and the global distortion of the contacting parts. The first is related to the local film thickness between the surfaces and its topography as well as the elasticity of the contacting surfaces. The second describes the compliance of the part itself, left hand side of equation (7), and is determined in overall elastic displacement calculation.

A real contact situation of rough surfaces around a single grid node is illustrated in Fig. 2. In the cross-sectional plane the pressure rise is shown in the interference area of the asperity summits. At high specific loads, a micro EHL solution on a single asperity summit shows, that the hydro-dynamic pressure can be approximated by the Hertzian pressure distribution. The nominal contact load for the grid element is derived by integration of the single contact pressures.

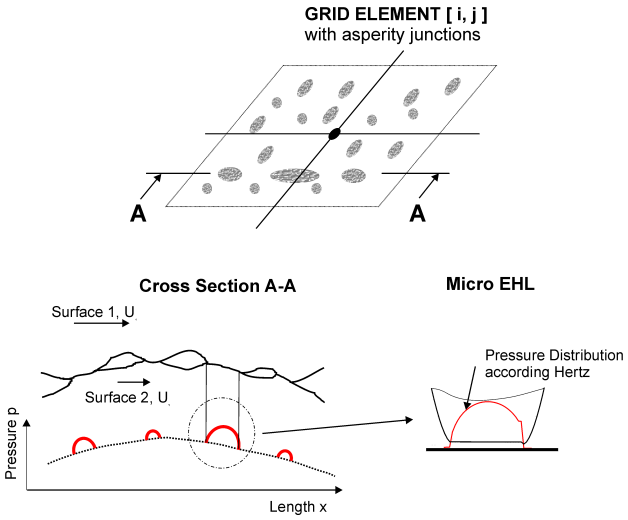

Figure 2: Mixed lubrication contact

Assuming Gaussian distribution for the surface roughness and asperity summits with constant radius of curvature the nominal contact pressure can be determined according to Greenwood and Tripp [9]:

$$p_a(h) = \frac{16\sqrt{2\pi}}{15}(\sigma_s \beta \eta)^2 E^* \sqrt{\frac{\sigma_s}{\beta}} \quad F_{5/2}(h/\sigma_s) \qquad (11)$$

Herein, h denotes the nominal film thickness, σ_s the summit height standard deviation, β radius at asperity summit and η surface density of asperity peaks. In the practical simulation those data are difficult to estimate. For that reason a simplified approach is used.

$$p_a(h) = K\, E^*\, F_{5/2}(h/\sigma_s) \qquad (12)$$

$$F_{5/2}(h/\sigma_s) = \begin{cases} 4.4086 \cdot 10^{-5}\,(4 - h/\sigma_s)^{6.804} & , h/\sigma_s < 4 \\ 0 & , h/\sigma_s \geq 4 \end{cases}$$

$$0.0003 < K < 0.003$$

The derived contact pressure function is superimposed by the hydrodynamic pressure function. Via integration, forces are calculated from the pressure field, that are applied to the grid nodes of the contacting bodies.

3 Simulation procedure

The simulation procedure consists of three main steps (Fig. 3):

- Pre-processing, including generation of geometry and structural matrices for each elastic body of the multi-body model using FEM, condensation, determination of external loads and generation of contact surface profile data for connected bodies
- Multi-body dynamics (MBD), considering vibro-acoustic analysis in time domain, contact dynamics between the elastic (rigid) bodies and external loads
- Post-processing including result extraction and body data recovery to the unreduced system

Stiffness and mass properties as well as geometry information can be generated using a commercial FE-software package (for results shown in this paper MSC-NASTRAN was used). The example for rigid body dynamics and elastic contacts was calculated by means of AVL-TYCON (equations in chapter 2.1) as described in [7, 8] and the method for elastic parts and mixed lubricated contacts is implemented in the software AVL-EXCITE (equations see chapter 2.2 and described in [4, 6]. In order to enable an efficient solution of vibration equations, a reduction (condensation) of the number of degrees of freedom has to be done.

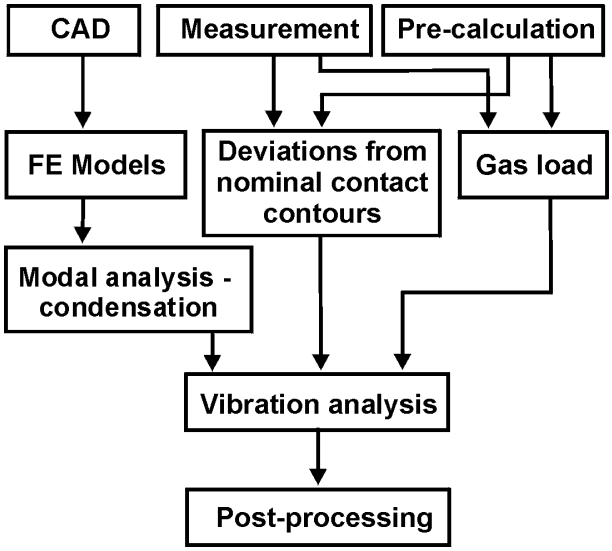

Figure 3: Flow chart for simulation procedure

Thus, the number of degrees of freedom (DoF) of the elastic parts can be reduced significantly (e.g. from 700000 to 2500 for a 4 cylinder engine). The reduced set $\boldsymbol{q}_a$ includes as well static as modal degrees of freedom and can be computed via

equation (13), where $\boldsymbol{G}_{fa}$ represents the transformation matrix:

$$\boldsymbol{q} = \boldsymbol{G}_{fa} \cdot \boldsymbol{q}_a \,. \tag{13}$$

Substitution of (13) in the equation of motion of a structural component, (7), and multiplication with the transposed transformation matrix $\boldsymbol{G}_{fa}^t$ from left hand side results in the reduced equation of motion of the component

$$\overline{\boldsymbol{M}} \cdot \ddot{\boldsymbol{q}}_a + \overline{\boldsymbol{D}} \cdot \dot{\boldsymbol{q}}_a + \overline{\boldsymbol{K}} \cdot \boldsymbol{q}_a = \bar{\boldsymbol{f}} \tag{14}$$

where $\overline{\boldsymbol{M}}$, $\overline{\boldsymbol{D}}$ and $\overline{\boldsymbol{K}}$ denote the condensed mass, damping and stiffness matrices and $\bar{\boldsymbol{f}}$ is the vector of condensed forces and moments. Vibration analysis is performed on the reduced system only.

In order to be able to consider forces and moments resulting from processes, that are not modelled within the calculation model directly (e. g. combustion), the corresponding data are included via time dependent load tables. These external loads can be pre-calculated or can be taken from measurement data.

Both the contact part geometry (e.g. piston) and the inner liner surface have not exact cylindrical contours. Beside the manufacturing profile of a piston skirt, the deviations from the nominal geometry result from gas loads as well as from thermal loads depending on the engine running condition. In addition, deformations due to assembly have to be considered in case of the liner structure.

Even if these deviations are in the range of a few microns, they can affect the hydro-dynamic calculation via the clearance gap function $\overline{h}$ and its derivative $\frac{\partial \overline{h}}{\partial t}$ significantly. Due to this, inaccurate contact surface profiles can lead to systematic errors in the calculation, affecting the results of as well global motions as vibration motions highly.

4 Validation Scenario

The complex models for the numerical simulation of noise generation mechanisms in engines need to be validated precisely. It makes sense to use this validation step for building up knowledge for uncertain parameters of the specific application models.

The challenge of such validation steps is due to the fact, that the primary components e.g. contact forces can not be measured, usually. Secondary components e.g. surface vibrations have to be used in stead.

4.1 Timing drive

As a first example the validation of the noise excitation generated by the chain of a timing drive of a recent 3 cylinder DOHC gasoline engine is shown, Fig. 4. The chain drive is equipped with a 8 mm bushing chain (130 links) the number of teeth at the crankshaft sprocket is 20. An automatic hydraulic chain tensioner combined with a tensioner arm is utilized to provide the required pretension.

The polygonal encasement of sprockets/guides by the chain causes a periodic fluctuation of the effective radius during sprocket's rotation, which leads to an excitation of longitudinal and transversal vibrations of the connected spans. Furthermore, the relative velocity measured in the contact direction between the chain's bush and sprocket's mesh leads to impacts, which occur periodically (1). Such effects appear with meshing frequency of the drive and are well known as "polygon effect".

Meshing-impacts and span vibrations are transferred via bearings, tensioner and guide mounts into the engine's structure. The excited structural vibrations are finally radiated as air borne noise. In cases where polygon-excitation matches with natural frequencies of the engine block, a significant whine noise can be recognized.

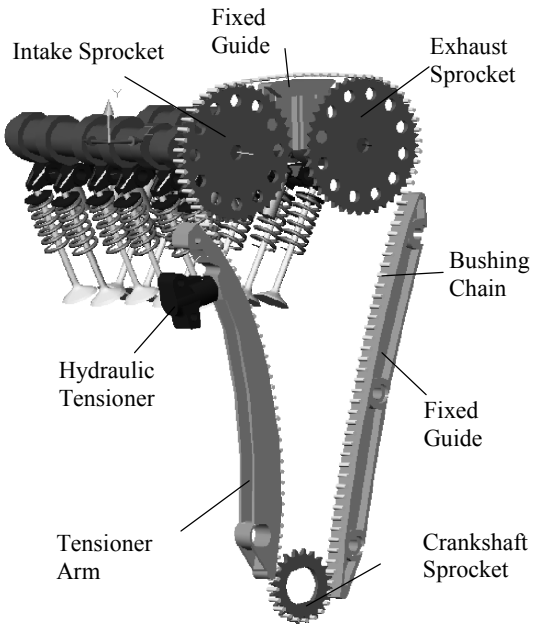

Figure 4: Timing drive of 3 cylinder DOHC gasoline engine

4.1.1 Simulation model

To simulate longitudinal/transversal vibrations and polygon-effect, a discrete 2D-model is applied (MBS equations as in chapter 2.1). Each chain-link is considered as a rigid body with three DoF's in its plane of motion. The chain's elastic/viscous behavior (incl. clearance) and friction in the joints is taken into account by force-units between the links.

Special contact elements based on a local stiffness/damping approach serve to consider the contact between chain-links and sprockets/guides, [7]. The implemented contact algorithm deals with the exact profiles at sprockets/guides and links, which is an absolute necessity when predicting meshing impacts. (s. Fig. 1).

Since the chain tensioner is one of the most important elements with regard to the chain drive's dynamic behavior, it must be modeled in detail. For that reason a combined hydraulic/mechanic-model is applied. Basically there are two main functions which have to be maintained by the chain tensioner; providing the required pre-load and introducing a sufficient amount of damping to the drive.

Torsional and bending behavior of the camshafts is taken into account by a discrete model consisting a series of 6 DoF rigid bodies connected with massless beam-elements. For the camshaft bearings an impedance method is applied to consider the non-linear characteristic of the oil gap.

Direct actuated finger followers are used for the actuation of the valves. The corresponding MBS-model contains all relevant parts like follower, hydraulic-lifter, valve (incl. valve seat) and valve spring. For the hydraulic lifter a hydraulic model is applied, valve spring is taken into account by a detailed multi-mass model including coil clash.

The entire model is described in detail in [7].

4.1.2 Validation results

The correct reproduction of the chain drive's primary dynamics is an absolute necessity when predicting structural excitations. To give an impression of the agreement with the experiment the angular velocity of the intake camshaft sprocket is examined.

The critical speed of this engine was found at 3400 rpm. At this speed the 1st natural frequency of the chain drive (about 85Hz) corresponds with the 1.5th engine order excitation. The natural frequency is rather low and mainly effected by the soft tensioner. Therefore, the tensioner behaviour was validated first in a separate test in order to adjust model parameters [8].

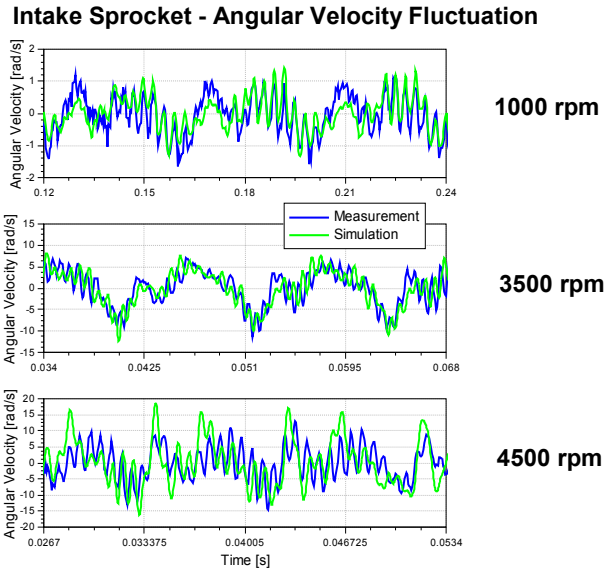

Figure 5: Comparison of calculated and measured angular velocities of the intake camshaft front

Final results are shown in Figures 5 and 6. Fig. 5 compares the results of calculated and measured fluctuations of the intake sprocket's angular velocity in time domain at three engine speeds. There is a good agreement, especially near resonance-speed (3500 rpm).

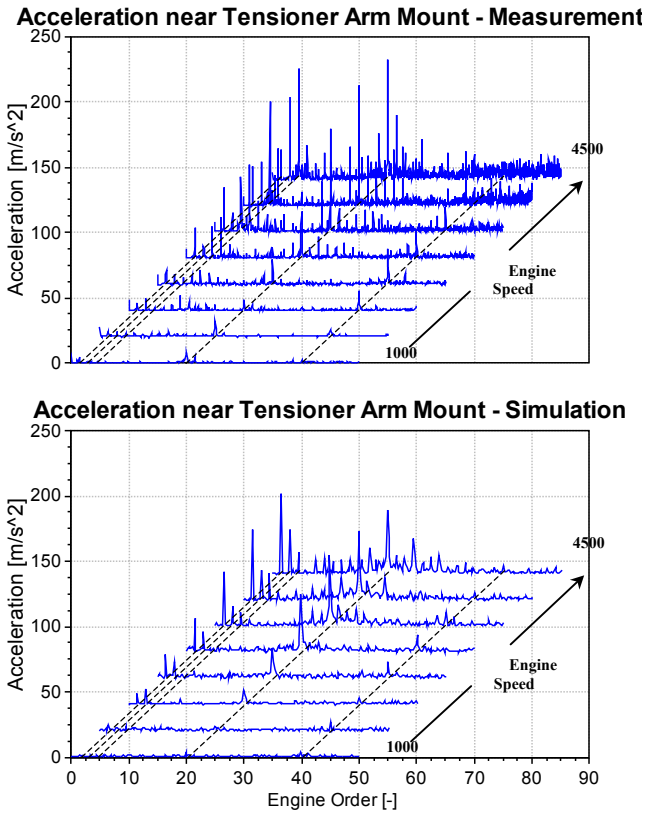

Figure 6: Comparison of calculated and measured accelerations near tensioner arm mount

After the validation of the dynamics of the rotating parts, structure borne excitation was investigated by comparing calculated and measured accelerations in the timing drive support. One example is shown in Fig. 6 for the accelerations near the tensioner arm mount. The correlation between calculation and test is very good again. Furthermore, main engine orders (1.5^{th} ,3^{rd} 4.5^{th}) and polygon order (20^{th}) as well as their 1^{st} harmonic (40^{th}) can be observed clearly in the order-traces in Fig. 6. In particular at medium engine speeds the polygon order is already one of the dominating frequencies. Thus, the tensioner arm mount can be identified as one of the important sources in view of whine noise excitation of the structure. One reason for the significant appearance of polygon order and related harmonics is the dominating viscous behaviour of the hydraulic chain tensioner, causing increased damping forces (and thus increased excitation) with increased relative velocities.

4.2 Piston slap

The second example is the validation of the noise excitation generated by the piston secondary motion after firing top dead centre (FTDC). In general, piston slap is one of several contributions to total engine noise. In specific engines and engine operating conditions it may become a dominating noise factor due to the significant frequency contents.

Therefore, the following simulation model has been developed in order to describe piston movement as well as the piston to liner contact and the transfer of structure borne noise to the block surface. Calculation and measurement were carried out for a turbo charged 4 cylinder truck diesel engine.

The piston slap noise excitation occurs due to the running clearance between piston and liner. After FTDC the piston changes from anti thrust to thrust side of the liner. The piston contact causes impact forces onto the liner and excites the entire engine structure. Effects on piston slap noise exist due to.

- running conditions of the engine
- contact geometry (piston and liner)
- con-rod ratio
- piston off-set
- amount of oil film in the contact
- structure stiffness
- piston mass, inertia and CG-position
- mass, stiffness and damping of the liner

4.2.1 Simulation model

The structural behaviour of the engine is modelled using the FE method. As the investigation is focused on piston slap and the relevant noise transfer path to the engine block surface, a specific part of the engine model was taken into account only. The simulation model consists of a complete model for the engine block (cylinder block and head, oil pan, etc.) with one piston installed in cylinder 4, as shown in Fig. 7. The relevant con-rod is connected to piston pin and crank shaft by non-linear spring-damper functions. The crankshaft is modelled via a one-node-body, rotating with constant speed.
The contact between piston and liner is modelled as a mixed lubrication joint as described in chapter 2.2.2. The number of degrees of freedom of the FE models is reduced by a condensation algorithm (as described in chapter 3) in order to reduce CPU time. The simulation is carried out in time domain based on software AVL EXCITE [4].

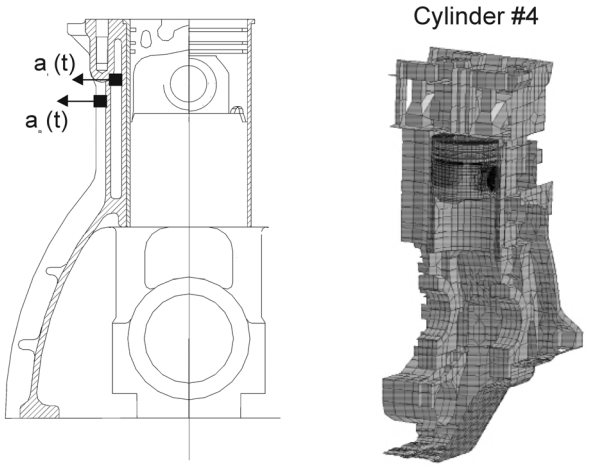

Figure 7: Accelerometers a(t) positions on the running engine (cylinder liner and block surface) and cross section of the FE model at cylinder #4.

4.2.2 Engine tests

The truck engine was measured in an anechoic chamber with several accelerometers installed on the engine block surface and at the cylinder liner. The two accelerometers used for this validation were positioned at cylinder liner and block surface in order to show significant responses on piston slap excitation at FTDC. At cylinder liner the slap event can be detected clearly while the block surface

response is reduced and filtered by the structure response and masked by several other excitation sources (combustion, crankshaft and timing drive, etc.). In the results for motored engine at 2000 rpm shown in Fig. 8 a, the piston slap event can be clearly observed at 0.3 ms after FTDC and causes a strong vibration excitation until 2.5 ms.

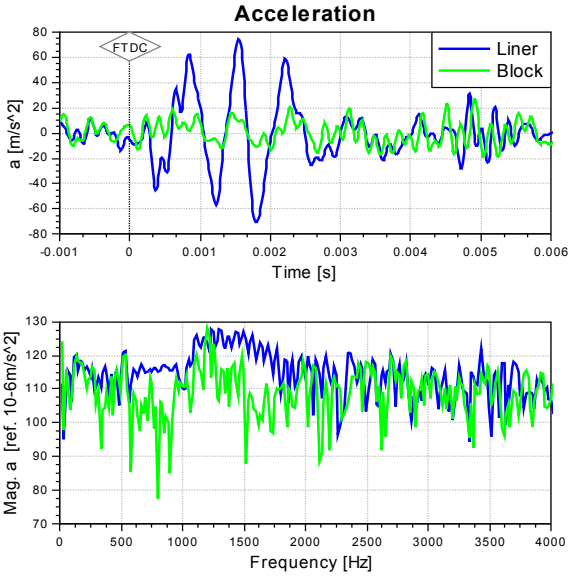

Figure 8: Comparison of structure accelerations for cylinder block and liner, 2000 rpm, motored engine.

4.2.3 Validation results

According to the results described above, 2000 rpm and motored engine condition are chosen as a suitable engine condition for the validation. It can be expected, that the effect of other noise sources on the validation at the liner is small.

Despite of having a detailed and precise simulation model, there are still remaining uncertain parameters due to unknown oil filling and exact local (warm) clearance between piston and liner in the running engine. To investigate these parameters, a broad in dept study was carried out.

The results in Figures 9 and 10 show the difference between measured and calculated results with and w/o the consideration of oil filling in the piston to liner contact gap. Both results in time and in frequency domains show to high vibration amplitudes, causing to much noise excitation in the simulation. It can be concluded, that the full mixed lubrication contact model (including oil lubrication) has to be used for a proper simulation of the piston slap noise excitation.

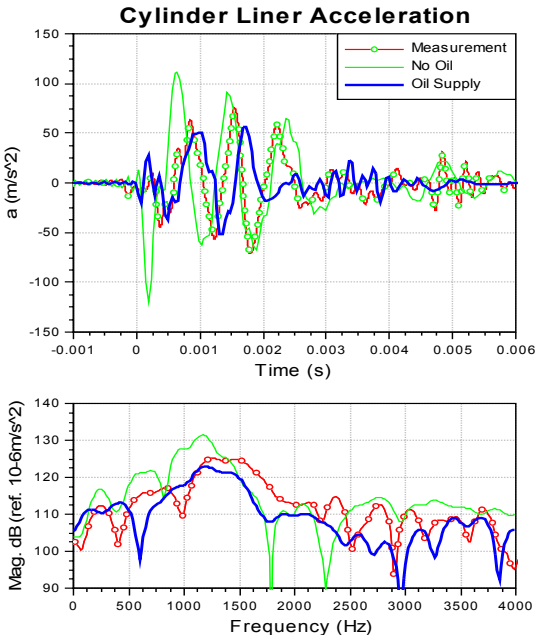

Figure 9: Comparison of measured and calculated accelerations at cylinder liner, zero minimum warm clearance (radial), 2000 rpm, motored engine

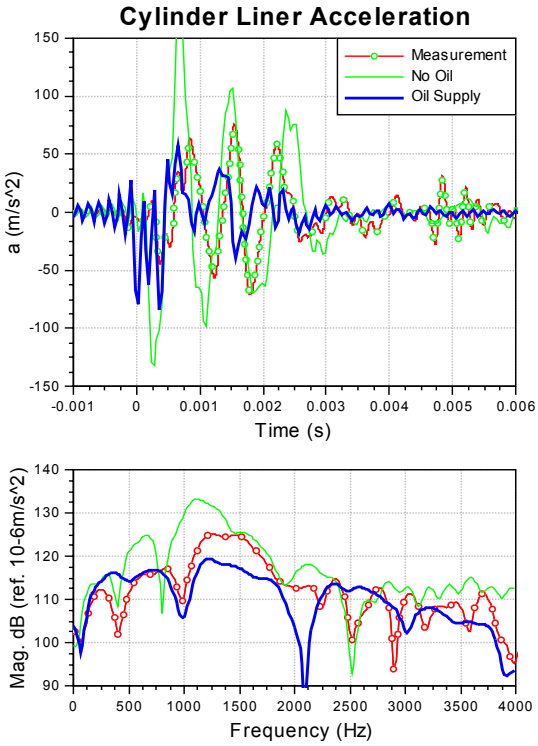

Figure 10: Comparison of measured and calculated accelerations at cylinder liner, 10 microns minimum warm clearance(radial), 2000 rpm, motored engine

Furthermore, the two Figures differ in the local minimum clearance occurring under warm conditions (minimum distance between piston and liner w/o deformations under load). For zero minimum clearance as in Figure 9, the correlation between measurement and calculation is much better in frequency domain as for a minimum clearance of 10 microns as considered for results in Figure 10.

5 Conclusions

Two typical examples of numerical simulation models for noise generation mechanisms in engines are described: The noise generated by the timing drive (chain drive) and the piston slap induced noise. The theoretical background for relevant mathematical models is given and the importance of the validation methodology is discussed in detail.

The following conclusions can be made:

- The specific contact models for structure borne noise excitation in combustion engines fulfil the required quality by showing the relevant physical events.
- Often, significant primary quantities e.g. contact forces and moments, can not be measured in engine tests directly. For systematic model improvement the validation of secondary quantities is required, e.g. surface accelerations, pressure in the tensioner, etc.
- Validation is a need for large and complex models in vibro-acoustics to build up modelling knowledge for specific applications. Thus, uncertain parameters can by studied and identified by successive comparision of measured and predicted results.
- The dynamics of engine components have to be correlated between test and calculation results first, before an assessment of the quality of structure borne noise excitation is reasonable.

Acknowledgements

This work was funded by the Austrian Government via the Christian Doppler Society. Measurement results were supported by IWIS Ketten, Joh. Winklhofer & Söhne GmbH&CoKG, Germany (example chain noise) and Acoustic Competence Center Graz (example piston slap noise).

References

[1] Priebsch H. H., Affenzeller J., Kuipers G.: *Prediction Technique of Vibration and Noise in Engines*, Proceeding, IMechE Conference Quiet Resolutions (1990)

[2] Richter B. (Editor): *Verbindung von MKS mit FEM-Modellen (Connecting MBD and FEM models)*, Haus der Technik e.V., Essen (1997)

[3] Priebsch H. H., Krasser J.: *Simulation of Vibration and Structure Borne Noise of Engines – A Combined Technique of FEM and Multi Body Dynamics,* CAD-FEM Users Meeting, Bad Neuenahr – Ahrweiler (1998)

[4] *AVL-Excite Reference Manual (Version 5.1)*, AVL LIST GmbH, Graz (1999)

[5] Offner G., Priebsch H. H.: *Elastic Body Contact Simulation for Predicting Piston Slap Induced Noise in IC Engines,* 2nd Trienial Intern. Symp. on Multi-body Dynamics, Bradford (2000).

[6] Priebsch H. H., Herbst H., Offner G.: *Piston Slap Induced Noise Simulation Considering Elasto-hydrodynamic Contact Conditions*, ASME Spring Techn. Conference, Philadelphia (2001)

[7] Sopouch M., Hellinger W., Priebsch H. H.: *Simulation of Engine's Structure Borne Noise Excitation due to the Timing Chain Drive*, Paper 2002-01-0451, SAE Congress, Detroit (2001)

[8] Sopouch M., Hellinger W., Priebsch H. H.: *Design Parameters of the Timing Chain Drive and their influence on Structure Borne Noise Excitation,* JSAE, Yokohama (2002)

[9] Greenwood, J. A., Tripp, J. H.: *The Contact of two Nominally Flat Rough Surfaces*, Proc. Instn. Mech. Engrs, Vol. 185 (1970-71)

[10] Gran, S.: *Mehrkörperdynamik elastischer Körper – Kurbeltrieb (Multi-body Dynamics of elastic bodies – Cranktrain)*, Theses, TU Graz (1994)